A proteomic analysis reveals that Snail regulates the expression of the nuclear orphan receptor Nr2f6 and IL-17 to inhibit adipocyte differentiation

Alberto Peláez-García[1], Rodrigo Barderas[2], Raquel Batlle[3], Rosa Viñas-Castells[3], Rubén A Bartolomé[1], Sofía Torres[1], Marta Mendes[1], María Lopez-Lucendo[1], Rocco Mazzolini[3], Félix Bonilla[4], Antonio García de Herreros[3], J. Ignacio Casal[1*]

[1]Department of Cellular and Molecular Medicine. Centro de Investigaciones Biológicas (CIB-CSIC). Madrid. Spain.
[2]Departamento de Biochemistry and Molecular Biology Department I, Universidad Complutense de Madrid. Spain
[3]IMIM-Hospital del Mar. Barcelona. Spain
[4]Hospital Puerta de Hierro. Majadahonda. Madrid. Spain

Running title: Snail1 induces IL-17 expression to inhibit adipogenesis

*Corresponding author:
J. Ignacio Casal
Department of Cellular and Molecular Medicine
Centro de Investigaciones Biológicas (CIB-CSIC)
Ramiro de Maeztu, 9
28040 Madrid. Spain
Phone: +34 918373112
Fax: +34 91 5360432
e-mail: icasal@cib.csic.es

Abbreviations

Cbx6, chromobox homolog 6; C/EBP, CCAAT/enhancer-binding protein; DAVID, Database for Annotation, Visualization and Integrated Discovery; EMT, epithelial-mesenchymal transition; IL-17, interleukin 17; mMSCs, murine mesenchymal stem cells; Nr2f6, orphan nuclear receptor 2f6; OsmR, oncostatin M receptor; PPAR, peroxisome proliferator-activated receptor; Prrx1, paired related homeobox 1 qPCR, quantitative PCR; RLU, relative luminescence units; SILAC, stable isotopic labeling amino acids in culture; TF, transcription factor; Trip4, thyroid hormone receptor interactor 4

SUMMARY

Adipogenesis requires a differentiation program driven by multiple transcription factors, where PPARγ and C/EBPα play a central role. Recent findings indicate that Snail inhibits adipocyte differentiation in 3T3-L1 and murine mesenchymal stem cells (mMSC). An in-depth quantitative SILAC analysis of the nuclear fraction of Snail-induced alterations of 3T3-L1 cells was carried out. In total, 2251 overlapping proteins were simultaneously quantified in forward and reverse experiments. We observed 574 proteins deregulated by Snail1 using a fold-change ≥1.5, with 111 up- and 463 down-regulated proteins, respectively. Among other proteins, multiple transcription factors such as Trip4, OsmR, Nr2f6, Cbx6 and Prrx1 were down-regulated. Results were validated in 3T3-L1 cells and mMSC cells by western blot and quantitative PCR. Knock-down experiments in 3T3-L1 cells demonstrated that only Nr2f6 (and Trip4 at minor extent) was required for adipocyte differentiation. Ectopic expression of Nr2f6 reversed the effects of Snail1and promoted adipogenesis. Since Nr2f6 inhibits the expression of IL-17, we tested the effect of Snail on IL-17 expression. IL-17 and TNFα were among the most up-regulated pro-inflammatory cytokines in Snail-transfected 3T3-L1 and mMSC cells. Furthermore, the blocking of IL-17 activity in Snail-transfected cells promoted adipocyte differentiation, reverting Snail inhibition. In summary, Snail inhibits adipogenesis through a down-regulation of Nr2f6, which in turn facilitates the expression of IL-17, an anti-adipogenic cytokine. These results would support a novel and important role for Snail and Nr2f6 in obesity control.

Keywords: Adipogenesis, obesity, Snail, Nr2f6, IL-17

INTRODUCTION

Adipogenic differentiation is driven by a complex cascade of transcription factors (TFs) and cell signaling molecules that lead to the expression of the master regulators CCAAT/enhancer-binding protein (C/EBP) (1) and peroxisome proliferator-activated receptor (PPAR) (2) family proteins. In a sequential process, C/EBPδ and C/EBPβ are initially induced and followed by C/EBPα and PPARγ expression. These two master TFs induce the final program of gene expression for adipocyte differentiation.

The transcription factor Snail1 is a major inducer of the epithelial-mesenchymal transition (EMT) during embryonic development and cancer progression (3, 4). Snail1 expression is very restricted in adult individuals (5), but reappears to drive the EMT process that confers pro-migratory, invasive and stem cell properties to cancer epithelial cells (4). During this process, Snail represses the expression of E-cadherin and promotes the expression of mesenchymal genes like vimentin. Recent reports indicate that Snail ectopic expression in murine mesenchymal stem cells (mMSCs) abrogated their differentiation to osteoblasts or adipocytes, whereas Snail depletion accelerated them (6). In addition, Snail1 knock-down caused a large decrease in the number of bone marrow mMSCs. This depletion comes accompanied of an acceleration of their differentiation to osteoblasts or adipocytes (6). Moreover, Snail1 regulates osteoblast differentiation through the inhibition of different proteins including Runx2 and vitamin D receptor (7), which indicates an antagonist role for Snail1 and vitamin D (8, 9).

The 3T3-L1 is a preadipocyte fibroblast cell line commonly used for the study of molecular mechanisms controlling adipogenesis (10, 11). Alike mMSCs, confluent 3T3-L1 preadipocytes differentiate to adipocytes upon exposure to a cocktail of adipogenic inducers (10). Upon adipogenic differentiation, Snail expression is almost

negligible in 3T3-L1 cells (12). Snail1 ectopic expression inhibits the adipocyte differentiation program (6, 12). Snail effect on adipogenesis was proposed to be mediated, among others, by activation of AKT (6) and was associated to an apparent inhibition of PPARγ and C/EBPα expression (12). Similar results were obtained in preventing the differentiation of bone marrow-derived murine mesenchymal stem cells (mMSC) to osteoblasts or adipocytes (6). Still, the molecular mechanisms underlying the effect of Snail on 3T3-L1/MSCs differentiation and the blocking of adipogenesis remain unclear.

Here, we investigated the transcriptional control by Snail1 blocking 3T3-L1 differentiation to adipocytes. To this end, we carried out an in-depth quantitative proteomic analysis of 3T3-L1 Snail-transfected cells using stable isotopic metabolic labeling (SILAC) (13). We focused our proteomic analysis on the nuclear fraction. In total, we identified 574 proteins deregulated, with most of them down-regulated by Snail1. To prove the general value of these findings, alterations were validated in mMSCs. Among others, we observed a direct repression of the orphan nuclear receptor Nr2f6, which in turn regulates expression of IL-17. These findings reveal a critical role for Nr2f6 and IL-17 to inhibit adipocyte differentiation. These results support an important function for Snail in obesity control.

EXPERIMENTAL PROCEDURES

Cell culture and adipocyte differentiation assays - Preadipocytes 3T3-L1 and mMSCs were stably transfected with 6 µg of either pcDNA3 Snail1-HA ("snail") or control pcDNA3 ("mock") using lipofectamine (Invitrogen). Cells were selected with G418 (1 mg/ml) for 3-4 weeks as described (6). Then, stably transfected 3T3-L1 and mMSC cells were grown in DMEM (Invitrogen) containing 10% FBS (Biological Industries), 1 mM L-glutamine, and 100 units/ml penicillin-streptomycin and supplemented with 0.5 µg/ml G418 at 37°C in 5% CO_2.

For adipocyte differentiation, 3T3-L1 cells were plated at a concentration of $1x10^6$ cells per well, in p60 plates, and cultured for 3 days. Differentiation was induced by the addition of 0.5 mM isobutyl-methyl-xanthine, 2 mM dexamethasone and 1.7 mM insulin. The induction medium was removed after 2 days and cells were supplemented with DMEM plus 10% FBS and 1.7 mM insulin and the medium was replenished after three days. When needed, cells were treated with anti-IL-17 antibody (500 ng/ml) (R&D Systems) every two days. For Oil Red O staining, cells were washed gently with PBS twice, fixed with 3.7% formaldehyde in PBS for 1 h at room temperature and stained for 1 h with filtered Oil Red O solution (1.8 mg/ml in 60% isopropanol). Solution was removed and plates rinsed with water and dried prior to image collection.

SILAC cell culture and nuclear protein extracts preparation - For metabolic labeling, 3T3-L1 Snail1 or control cells were grown and maintained in DMEM containing either light L-lysine and L-arginine or heavy [$^{13}C_6$]-L-lysine and [$^{13}C_6$]-L-arginine (Dundee Cell Products) supplemented with 10% dialyzed FBS, 100 units/mL of penicillin/streptomycin and 0.5 µg/ml G418 at 37ºC in 5% CO_2. Eight duplications

were necessary to achieve >97% incorporation of the heavy amino acids (14) calculated for individual proteins as previously described (15). We carried out forward and reverse experiments to get a biological replicate and avoid labeling bias in the study.

For nuclear protein extraction, cells were washed twice with chilled PBS, resuspended with PBS containing 4 mM EDTA, and harvested by centrifugation at 500*g* for 5 min. Then, we used the "Subcellular protein fractionation kit" (Pierce). Protein quantification was performed using the tryptophan method (16). Then, 25 µg of protein from nuclear cell extracts were mixed at a 1:1 ratio and run at 25 mA per gel in 12.5% SDS-PAGE. Gels were stained with colloidal coomassie blue and lanes were cut into 18 slices. Excised bands were cut into small pieces and destained with 50 mM ammonium bicarbonate/50% acetonitrile (ACN), dehydrated with ACN and dried. Gel pieces were rehydrated with 12.5 ng/µL trypsin in 50 mM ammonium bicarbonate and incubated overnight at 30ºC. Peptides were extracted at 37ºC using ACN and, then 0.5% TFA, dried, cleaned using ZipTip with 0.6 µl C18 resin (Millipore) and reconstituted in 5 µL 0.1% formic acid/2% ACN, prior to MS analysis, which was performed as previously described (17).

Mass spectrometry analysis, protein identification and SILAC quantification - Peptides were trapped onto a 2 cm C18-A1 ASY-Column (Thermo Scientific), and then eluted onto a Biosphere C18 column (10 cm long, inner diameter 75 µm, 3 µm particle size) (NanoSeparations) and separated using a 170 min gradient from 0-35% Buffer B (Buffer A: 0.1% formic acid/2% ACN; Buffer B: 0.1% formic acid in ACN) at a flow-rate of 300 nL/min in a nanoEasy HPLC (Proxeon) coupled to a nano-electrospray ion source (Proxeon). Mass spectra were acquired on an LTQ-Orbitrap Velos mass

spectrometer (Thermo-Scientific) in the positive ion mode. Full-scan MS spectra (m/z 400-1200) were acquired in the Orbitrap with a target value of 1,000,000 at a resolution of 60,000 at m/z 400 and the 15 most intense ions were selected for collision induced dissociation (CID) fragmentation in the linear ion trap with a target value of 10,000 and normalized collision energy of 35%. Precursor ion charge state screening and monoisotopic precursor selection were enabled. Singly charged ions and unassigned charge states were rejected. Dynamic exclusion was enabled, with a repeat count of 1 and exclusion duration of 30s. Mass spectra (*.raw) files were searched against the SwissProt mouse database 57.15 (16230 sequences) using MASCOT search engine v. 2.3 (Matrix Science) through Proteome Discoverer (version 1.4.1.14) (Thermo). Search parameters included a maximum of two missed cleavages allowed, carbamidomethylation of cysteines as a fixed modification and oxidation of methionine, N-terminal acetylation and ^{13}C-Arg, ^{13}C-Lys as variable modifications. Precursor and fragment mass tolerance were set to 10 ppm and 0.8 Da, respectively. Identified peptides were validated using Percolator algorithm with a q-value threshold of 0.01. For each SILAC pair, Proteome Discoverer determines the area of the extracted ion chromatogram and computes the “heavy/light” ratio. Protein ratios are then calculated as the median of all the unique quantified peptides belonging to a certain protein. The ratios among proteins in their heavy and light versions were used as fold-change. Proteins were quantified with at least one peptide hit in forward and reverse experiments. The fold change cutoff for deregulated proteins was calculated using a permutation-based test as described (18). Proteins with quantification variability >20% were manually inspected by checking the isotopic envelope of both heavy and light forms and how many peaks of the envelope were used to determine the area of the

envelope of all PSMs corresponding to the peptides used to identify the protein. A multipoint normalization strategy was applied to normalize the data sets against the 5% trimmed mean values, which is a robust statistical measure of central tendency that normalize most of the $\log_2$ protein ratios to 0. Briefly, the 5% of the most extreme outliers –values- were removed and the mean of the 95% remaining data was determined, and used to normalize the ratio values, and thus, minimizing the effect of these extreme outliers and centering the $\log_2$ ratio distribution to zero. Since metabolic conversion arginine/proline can affect quantification accuracy in some cell types, we investigated arginine to proline conversion in 3T3-L1 cells. Using heavy proline as a variable modification, less than 1% of proline-containing peptides were heavy labeled in 3T3-L1 cells. The mass spectrometry proteomics data have been deposited to the ProteomeXchange Consortium (19) via the PRIDE partner repository with the dataset identifier PXD001529.

Western blot analysis - Protein extracts from 3T3-L1 and mMSC cells were prepared as described (20). Briefly, 25 µg of each protein extract were run in parallel using 10% SDS-PAGE. For immunoblotting, proteins were transferred to nitrocellulose membranes (Hybond-C extra) using wet transfer (Bio-Rad). After blocking, membranes were incubated at optimized dilutions with primary antibodies followed by incubation with either HRP-anti-mouse IgG (Pierce) or HRP-anti-rabbit IgG (Sigma) at 1:5000 dilution. Specific reactive proteins were visualized with SuperSignal West Pico Maximum Sensitivity Substrate (Pierce). Snail antibody was used as described (5). A total of 21 different antibodies were used (supplementary Table S1).

RNA extraction, semi-quantitative and real-time quantitative PCR - RNA was extracted from cell lines with the RNeasy Mini Kit (Qiagen) and quantified with a NanoDrop ND-1000 spectrophotometer (NanoDrop Technologies Inc.). cDNA was synthesized using the Superscript III First Strand Synthesis kit (Invitrogen). For semiquantitative reverse transcriptase-PCR (RT-PCR), reactions were performed using specific primers for each gene (supplementary data 1), the PCR products were separated on 2% agarose gel and stained with GelRed (Biotium). Quantitative PCR (qPCR) analysis was performed using specific primers (supplementary data 1) and SYBR-Green Master PCR mix (Bio-Rad) in triplicate. Data collection was performed on an IQ5 (BioRad). All quantitations were normalized using mouse 18S rRNA as internal control.

Luciferase assay - Different promoter regions were obtained by PCR amplification. Primers were designed to generate fragments of approximately 1000 bp (Supplementary data 1). In all cases, the reverse primers were at positions: +277/+297. The amplified fragments were: pTrip4 -650/+277, pNr2f6 -700/+269, pOsmR -700/+297, pPrrx1 -680/+287 and pCbx6 -681/+293. They were digested using *Mlu*I and *Xho*I restriction sites, inserted into pGL3-Luc and sequenced. We used a pGL3 vector containing the -178 / +92 fragment of the E-cadherin (CDH1) promoter as a reference. Luciferase protein expression, in terms of relative luminescence units (RLU), was determined using a luciferase assay kit (Promega) at 24h post-transfection using a Glomax Reader (Promega). Luciferase expression in all transfections was calculated and normalized with the protein content and expressed as RLU per µg. The protein content was determined using the 2D-Quant kit (GE Healthcare).

Chromatin imunoprecipitation assay - ChIP experiments were performed as described (21). Briefly, mMSC-Snail cells were cross-linked with 1% formaldehyde for 10 min at 37ºC. Cross-linking was stopped by adding 0.125 M glycine for 2 min at room temperature. Cell monolayers were scraped in cold lysis buffer (50 mM Tris, pH 8.0, 10 mM EDTA, 0.1% NP-40, and 10% glycerol), and incubated 20 min on ice. Nuclei pellets were lysed with 1% SDS, 10 mM EDTA and 50 mM Tris, pH 8.0 and extracts were sonicated. Supernatants were diluted 1:10 with dilution buffer, and immunoprecipitation was done overnight at 4ºC using an anti-Snail antibody or an irrelevant antibody. DNA was purified with GFX kit (GE Healthcare) and eluted in MilliQ water. Promoter regions were analysed by quantitative PCR with SybrGreen staining (Roche) using the oligonucleotides indicated in supplementary data 1.

siRNA transfections - siRNAs for Snail1, Nr2f6, Prrx1, Trip4, Cbx6 and controls were purchased from Sigma. For siRNA transfections, cells were transfected with 27.5 pmol siRNA using 1 µl JetPrime Transfection reagent (Polyplus Transfection) in 100 µl of JetPrime buffer. Then, cells were grown in p60 culture plates with complete culture medium and used as indicated. For adipocyte differentiation assays after siRNA transfection, cells were grown 48 h with complete culture medium after transfection and, then, adipocyte differentiation was performed as above.

Cloning and transfections of Nr2f6 - Nr2f6 cDNA (clone # MGC:6088 IMAGE:3582557) was obtained from the IMAGE-MGC collection. The cDNA was amplified by PCR with the Advantage 2 polymerase (Clontech) using the primers: 5'-AGGAATTCATGGCCATGGTGACCGGT-3' and 5'-

CGCGGTACCCTAGCCCGAGCCATAGGG-3'. The PCR product was digested with *EcoR*I and *Kpn*I and cloned into pcDNA3.1 (Invitrogen). Nr2f6 cloning was confirmed by DNA sequencing. Cells were transfected with pcDNA3.1/Nr2f6 or empty vector using JetPrime. After 24-48h, transiently transfected cells were lysed and the expression of Nr2f6 was analyzed by western blot and qPCR.

Cell proliferation - For cell proliferation assays, experiments were carried out using MTT (3-(4,5-dimethylthiazol-2-yl)-2,5-diphenyltetrazoliumbromide) (Sigma) as described (22).

Cytokine array and ELISA - Conditioned medium from 3T3-L1 or mMSC cells, mock or Snail1-transfected, was collected after 48 h in serum-free medium and incubated with the Mouse Cytokine Antibody Array 3 containing 62 murine cytokine specific antibodies. Then, membranes were scanned and analyzed using Redfin, a 2D-gel image analysis software (Ludesi) as described (23). Relative cytokine intensities were normalized in comparison to control spots on the same membrane and represented in arbitrary units. Individual quantification of murine IL-17 was carried out with an ELISA kit (RayBiotech).

Bioinformatics and statistical analysis - Ingenuity Pathway Analysis (IPA) (Ingenuity Systems) was used to predict biological functions and protein interaction analysis. DAVID Database was used to evaluate the enrichment of nuclear proteins in our proteomic dataset (24). For evaluation of the statistical significance compared between groups, all *p* values were derived from a two-tailed statistical test with 95% confidence

interval. *p* values <0.05 were considered statistically significant. All statistical analyses were done with Microsoft Office Excel.

RESULTS

Protein alterations in nuclear extracts of Snail1-transfected 3T3-L1 -

Overexpression of Snail1 in 3T3-L1 and mMSC cells was confirmed by western blot (Fig. 1*A*). For comparison purposes, we tested Snail1 and the active fibroblasts marker S100A4 expression at different confluence levels (50, 80 and 100%). As fibroblast activation depends on cell-cell contact, Snail1 expression increased gradually and was maintained 48h after confluence, conditions suitable for these cells to be differentiated to adipocytes. These conditions were selected for proteomic analysis (Fig. 1*B*). 3T3-L1 cells (Snail-transfected and mock) were metabolically labeled in SILAC medium for at least 8 doublings. Then, labeled cells were synchronized to get 100% confluence at the same day and 48h later were collected for nuclear subproteome analysis (Fig. 1*C*). Quality of the cell fractionation was confirmed by western blot using antibodies against nuclear protein Lamin B and cytoplasmic Rho GDI (Fig. 1*D*). Two biological replicates were carried out. We identified 3920 proteins using forward and reverse SILAC experiments, with 2800 overlapping nuclear proteins in 3T3-L1 cells (Fig. 1E). In total, 3483 proteins were quantified in the forward and reverse experiments, with 2251 proteins quantified in common (Fig. 1E). Representative mass spectra showed a correct incorporation of the heavy labeled amino acids (supplementary Fig. S1). By using a permutation-based statistical test, we fixed a fold-change ≥ 1.5 (mean of two experiments) as significant. For a few proteins fulfilling the fold-change requirement but with a variability >20%, MS/MS spectra were manually inspected (supplementary Fig. S2). We found 574 proteins deregulated by Snail1 in the nuclear fraction of 3T3-L1 cells, with 111 and 463 up- and down-regulated proteins, respectively

(supplementary Table S2). Using DAVID, we observed a significant enrichment in nuclear proteins, 458 out of 2251 quantified proteins in 3T3-L1 (Fig. 1F).

Network and pathways alterations induced by Snail - Among other functions, Snail-deregulated proteins were involved in chromatin remodeling such as Hmga2, Top2A (up-regulated) or chromobox proteins such as CBX1, 3, 5 (up) 6 and 8 (down-regulated) (Fig. 2*A*) (Table I**)** (Supplemental Table S2). Most of the quantified proteins were down-regulated such as OsmR (oncostatin M receptor) and transcription factors like Stat1, Stat3, NFkB, Trip4, Nr2f6, Prrx1 and Sra1 (a component of the ribonucleoprotein complex coactivator NCOA1). Src-related proteins, such as c-Src, Fam120A, Sh3bp1, Lipb1 and Tln1 were also down-regulated, as well as β-catenin, Gsk3β, Rsk6 and Yap1, which have been described to inhibit cell differentiation**.**

Ingenuity Pathway Analysis (IPA) database was used to identify the predicted pathways and biological functions most significantly altered due to the ectopic expression of Snail. The mTOR pathway, EIF2 signaling, RAN signaling, PI3/AKT signaling, integrin and cytokine/chemokine signaling were among the top altered pathways (Fig. 2*B*). Regarding adipogenesis mediators, Snail caused an increase in the levels of C/EBPβ in 3T3-L1. In addition, IPA predicted a down-regulation of PPARγ and up-regulation of C/EBPβ based on proteomics data of other 47 deregulated proteins associated to adipogenesis in 3T3L1 (Fig. 2*C*). The increase of C/EBPβ suggests that Snail expression did not affect the initial phases of differentiation. This would agree with the increase in the replication capacity of Snail cells and could explain the capacity of Snail-expressing fibroblasts for sarcomagenesis (25).

Validation and analysis of adipogenesis-related proteins - An initial validation of Snail-deregulated proteins was performed by PCR and western blot in 3T3-L1 and mMSC cells. First, we tested those genes of the C/EBP and PPAR families involved in adipogenesis. By PCR, we confirmed the increase in C/EBPβ and the lack of expression of PPARγ and C/EBPα in non-differentiated Snail-transfected cells (Fig. 3*A*). The down-regulation of Cbx6, Nr2f6 and, particularly, Prrx1 was confirmed by qPCR in both cell types 3T3-L1 and mMSC cells (Fig. 3B). In contrast, expression of Trip4 and OsmR was not decreased by Snail in mMSC cells, which might be associated to the stem-like properties of mMSC cells respect to the more differentiated status of the 3T3-L1 cell line.

By western blot, we confirmed the down-regulation of phosphoRPS6, phospho mTOR and eIF3D for mTOR signaling, Akt, pAkt, Stat3, pStat3, Fam120A, Talin1, pSrc and Src for cell signaling alterations and transcription factors Yap1, Sra1, Prrx1, Trip4, Nr2f6 and Cbx6 (Fig. 3C). In general, differences were more visible in 3T3-L1 than in mMSC cells, probably due to the higher expression of Snail1 in 3T3-L1 transfected cells. We also confirmed the activation of phosphoAkt in Snail-expressing cells as previously reported (6). Akt phosphorylation was observed at Ser-473, which is regulated by mTORC2 activation (26). This result suggests that the observed mTOR inhibition corresponds mainly to mTORC1, involved in RPS6 and not in Ser-473Akt phosphorylation. Moreover, as a consequence of mTORC1 down-regulation, the eIF3 complex and other downstream regulators of mTORC1-RPS6 pathway such as RPS6 and Erk1 were also down-regulated in Snail1-transfected cells (27, 28).

Snail1 causes a direct regulation of multiple transcription factors - *In silico* analysis with MatInspector revealed putative Snail1 E-box consensus motifs in 28 promoters of the quantified proteins (Supplemental Table S3). We focused our study on TFs modulated by Snail. To analyze the effect of Snail on these TFs, we carried out a luciferase assay using the repression of the E-cadherin promoter as a control (Fig. 3D). Snail inhibited the luciferase promoter activity for Trip4, Nr2f6, OsmR and Prrx1 genes, and only slightly that for Cbx6. Compared to E-cadherin, highest repression was observed for Prxx1 and Trip4, similar for Nr2f6 and lower for Cbx6 and OsmR.

The binding of Snail to the promoters of these transcription factors was confirmed using a ChIP assay. Chromatin samples were immunoprecipitated with a specific antibody against Snail1 in comparison to an irrelevant antibody as control. We used PTEN as positive control of Snail regulation (6, 21). Snail was recruited to all the tested promoters containing E-box motifs, showing a greater binding for Trip4, Nr2f6, OsmR and Prrx1 than for PTEN and not for Cbx6 (Fig. 3E). Finally, we tested whether Snail silencing in 3T3-L1 and mMSC cells transfected with Snail down-regulated the expression of these TFs (Fig. 3F). Although the silencing of Snail was not complete, there was a clear increase in Nr2f6 and Trip4, and, particularly, Prrx1 in both cell types. Collectively, these results demonstrate a direct regulatory effect of Snail on the promoters of Nr2f6, Trip4 and Prrx1.

Down-regulation of Nr2f6 controls adipogenic differentiation - To further evaluate the role of these TFs on adipocyte differentiation, we knocked down Prrx1, Nr2f6, Trip4 and Cbx6 expression in wild-type 3T3-L1 cells using specific siRNAs. Changes in lipid content after culturing cells with differentiation cocktail were detected visually

in entire culture plates and microscopically representative fields (Fig. 4*A*) or quantitatively by colorimetry of Oil Red staining (Fig. 4*B*). There was a strong inhibitory effect caused by the loss of Nr2f6 in adipocyte differentiation. Trip4 effects were minor, but still significant. Snail1 expression levels remained unaffected after Nr2f6 silencing (Fig. 4*C*). In addition, an increase of Nr2f6, maintaining similar Snail1 expression levels, was observed during 3T3-L1/Snail differentiation (Fig. 4*D*). By qPCR, the levels of Nr2f6 and the master adipogenic mediators PPARγ and C/EBPα were down-regulated by Snail1 expression when compared to 3T3-L1 mock cells, except C/EBPβ that was not repressed by Snail (Fig. 4*E*). Collectively, these results suggest an important role for Nr2f6 in adipocyte differentiation.

Overexpression of Nr2f6 promotes adipogenesis - Conversely, to further address the positive role of Nr2f6 in adipogenesis, we ectopically expressed Nr2f6 in 3T3-L1/Mock and 3T3-L1/Snail cells. We adjusted conditions of transfection (1 µg/ $5x10^6$ cells) to avoid an excessive cell death caused by Nr2f6 overexpression. Enhanced expression of Nr2f6 did not alter Snail1 levels of expression as detected by Western Blot and qPCR (Fig. 5*A*-*B*). By qPCR, we observed a large increase of expression of Nr2f6 in transfected cells accompanied by an important increase of C/EBPα and C/EBPβ in 3T3-L1/Mock cells. Snail1 ectopic expression greatly inhibited the up-regulation of C/EBPα. Meanwhile, PPARγ remained down-regulated in both types of cells, suggesting that additional factors, different from Nr2f6, might be contributing to its regulation (Fig. 5*B*). During adipocyte differentiation, overexpression of Nr2f6 in 3T3-L1/Mock cells increased the accumulation of lipid droplets and accelerated their differentiation in comparison to non-transfected cells (Fig. 5*C*-*D*). Visualization of culture plates and

quantification of extracted Oil Red O absorbance accumulated in 3T3L1/Mock cells confirmed that enhanced expression of Nr2f6 increased significantly adipogenesis (Fig. 5*D*). Excessive cell death caused by ectopic expression of Nr2f6 in Snail-transfected 3T3-L1 cells made impossible to carry out differentiation experiments in these conditions. Finally, overexpression of Nr2f6 caused a lower proliferation rate of 3T3-L1/Mock cells, in contrast with the highly proliferative rate induced by Snail1 (Fig. 5*E*). This lower proliferation might be associated to the increase in cell death caused by the enhanced expression of Nr2f6.

Snail expression induces the synthesis of IL-17 - The nuclear orphan receptor Nr2f6 is a repressor of IL-17 expression, suppressing Th17 cell functions (29). IL-17 inhibits adipogenesis downstream of C/EBPδ and C/EBPβ and upstream of C/EBPα and PPARγ (30). To determine if the effect of Nr2f6 on adipogenesis was mediated by IL-17, we checked the levels of IL-17 and other cytokines analyzing conditioned medium of Snail-transfected and mock cells using a cytokine-specific microarray. After densitometry and quantification, we observed a significant difference for IL-17 and TNFα between Snail-expressing and mock cells (Fig. 6*A*). To confirm these results, we quantified IL-17 by ELISA using the same cells and the results were similar to that obtained with the array (Fig. 6*B*). Moreover, IL-17 expression was increased in Nr2f6-silenced cells and decreased in cells ectopically expressing Nr2f6 (Fig. 6*C*). To study the effect of blocking IL-17 activity on adipogenesis, Snail1-expressing 3T3-L1 cells were treated with anti-IL17 antibody (500 ng/ml) every two days upon addition of the adipogenic cocktail. Despite the relatively low antibody concentration, treated cells showed a significant recovery of differentiation capacity, visually and by colorimetry (Fig. 6*D*).

Collectively, these results demonstrated a capacity of mesenchymal cells to secrete IL-17 and inhibit adipocyte differentiation upon Snail expression and the concomitant loss of Nr2f6.

DISCUSSION

By using a sensitive and quantitative proteomic analysis, we identified a number of transcription factors, cytokines and growth factors deregulated by Snail. The capacity of Snail to bind and regulate the selected transcription factors was confirmed by luciferase and ChIP assays. We provide diverse evidences that Snail regulates adipocyte differentiation in mesenchymal cells through the inhibition of the nuclear orphan receptor Nr2f6, which antagonizes the expression of the pro-inflammatory cytokine IL-17 (31). Snail overexpression induced IL-17 as well as TNFα secretion in 3T3-L1 and mMSCs. We demonstrated that enhanced expression of Nr2f6 or blocking of IL-17 activity enabled the recovery of adipocyte differentiation. Collectively, our results suggest an early effect of Snail on adipogenesis mediated through Nr2f6 and IL-17 that occurs upstream of C/EBPα and PPARγ proteins (Fig. 7).

Our proteomic data of Snail-transfected cells agree with the up-regulation of C/EBPβ induced by IL-17 and associated to early differentiation of adipogenesis (32, 33). Exogenous IL-17 inhibited 3T3-L1 adipogenesis (34) through C/EBPα, PPARγ and Kruppel-like factors (30). However, no insights about the provenance of this IL-17 were given or the reasons behind the presence of a Th17 cytokine in the differentiation of mesenchymal cells to adipocytes were explained. Another report suggested a direct repression of PPARγ by Snail based on a luciferase assay (12). However, to the light of our results and the capacity of Snail to bind multiple promoters, it is difficult to know if PPARγ inhibition by Snail is functionally relevant in 3T3-L1 cells or is another unspecific repressor capacity of Snail. In fact, C/EBPα and PPARγ expression levels were very low in both, mock and Snail-transfected cells. Curiously, C/EBPα and C/EBPβ expression was increased in Nr2f6 transfected 3T3-L1 cells, whereas the levels

of Snail were not affected. This increased expression of C/EBPα and C/EBPβ would support an acceleration of the differentiation program.

IL-17 is usually classified as a proinflammatory cytokine, which is known to control bone mass (7) and to inhibit osteoclast formation (35) and chondrocyte differentiation (36). Here, we propose a novel capacity for Snail to induce IL-17 expression in fibroblasts or mesenchymal cells. In fact, we may speculate that previously reported inhibitory effects of Snail on osteoblast differentiation (6) were also caused by IL-17. Therefore, the action of fibroblast-derived IL-17 would be more far-reaching than that restricted to Th17 cells and might contribute to the Snail regulation of cancer microenvironment. This capacity of Snail to regulate IL-17 expression suggests a role for this molecule in different pathologies as obesity, rheumatoid arthritis or osteoporosis. Since Snail and TGFβ form a self-stimulatory loop, either Snail or TGFβ could be interesting targets on these diseases.

Our results for Nr2f6 are relatively similar to those described for Nr2f2 (also known as COUP-TFII) in adipogenesis (37) and may suggest a cooperative interaction between both nuclear orphan receptors (Fig. 7). However, the role of Nr2f2 in adipogenesis is controversial as Xu et al (38) described the opposite effect for Nr2f2. In our dataset, Snail showed a very weak repressor effect on Nr2f2 (mean fold-change: 0.934) (data not shown). According to the Nr2fome database (39), Nr2f6 (also known as Ear2) interacts and regulates a number of nuclear receptors, among others Nr2f2, Esr1(Estrogen Receptor) or Angptl1. Although Nr2f6 has been much less characterized than Nr2f2, it has been described that both are functionally closely related. However, whereas Nr2f2 knockout mice are lethal, Nr2f6 are viable but present some neurological disorders (40). Nr2f2 is a central node between Nr2f6, Trip4 and other proteins like

elongation factors (41, 42) (**Fig. 7**). In addition, Esr1 interacts with Nr2f6 and C/EBPα, C/EBPβ, RARA, STAT3, STAT5, Trip4 and Sra1, among many other TFs (43). Many of these nuclear receptors are also involved in IL-17 expression like VDR, RAR, ER and LXR (31).

Another TF regulated by Snail that showed a minor effect on adipogenesis was Trip4. Trip4, also called activating signal cointegrator 1 (Asc1), is a transcription coactivator of nuclear receptors that plays a pivotal role in the transactivation of NFκB and AP1 (44). Trip4 also regulates androgen receptor transactivation and testicular function (45, 46). Trip4 has been described to interact also with PPARγ (47). In addition, Snail1 expression caused a down-regulation of the homeobox factor Prrx1, an inducer of the epithelial-mesenchymal transition (EMT). Prrx1 causes a reversion of the EMT process in cancer epithelial cell lines, apparently without Snail participation (48). In contrast, we observed a direct repression of Prrx1 by Snail in preadipocyte 3T3-L1 and mMSC cells, confirmed by luciferase and ChIP assay, although silencing of Prrx1 did not affect adipogenic differentiation. Other down-regulated protein was the steroid receptor RNA activator (Sra1), which promotes adipocyte differentiation; up-regulates the expression of PPARγ, C/EBPα and other adipocyte genes; and increases glucose uptake and phosphorylation of Akt and FOXO1 in response to insulin (49). Here, we have noticed a clear down-regulation of Sra1 that might contribute also to the suppression of PPARγ and adipocyte differentiation. Sra1 is also a component of a large complex with Nr2f6 according to the Nr2fome.

In summary, many of the Snail-regulated TFs (Nr2f6, Trip4 or Sra1) seem to interact, directly or indirectly, with PPARγ. However, Nr2f6 repression showed the stronger capacity to control adipocyte differentiation via IL-17. At the end, IL-17 seems

to be the critical mediator induced by Snail for adipocyte differentiation. These results support a link between Snail1 expression, inflammation and adipogenesis. Snail appears to be a master regulator that plays a central role at different levels to favor the expression and/or repression of a cascade of multiple transcription factors that control adipogenic gene expression at different levels. Further work is required to precisely define the interaction network between other identified transcription factors. These results provide a functional role for Snail in obesity that goes beyond the control of the EMT process and epithelial plasticity.

ACKNOWLEDGEMENTS

Alberto Peláez-Garcia is recipient of a FPI fellowship. Rodrigo Barderas is supported by the Ramón y Cajal Programme of the MINECO. R.A. Bartolomé is supported by a grant to established research groups of the Asociación Española Contra el Cáncer (AECC). S. Torres is a recipient of a Juan de la Cierva programme. This research was supported by a grant to established research groups (AECC), grant BIO2012-31023 from the Ministry of Economy and Competitiveness, grant S2011/BMD-2344/ (Colomics2) from Comunidad de Madrid and ProteoRed-ISCIII support. Work at AGH's lab was supported by a grant from the Ministry of Economy and Competitiveness (SAF2010-16089).

REFERENCES

1. Freytag, S. O., Paielli, D. L., and Gilbert, J. D. (1994) Ectopic expression of the CCAAT/enhancer-binding protein alpha promotes the adipogenic program in a variety of mouse fibroblastic cells. *Genes Dev* 8, 1654-1663

2. Tontonoz, P., Hu, E., and Spiegelman, B. M. (1994) Stimulation of adipogenesis in fibroblasts by PPAR gamma 2, a lipid-activated transcription factor. *Cell* 79, 1147-1156

3. Barrallo-Gimeno, A., and Nieto, M. A. (2005) The Snail genes as inducers of cell movement and survival: implications in development and cancer. *Development* 132, 3151-3161

4. Peinado, H., Olmeda, D., and Cano, A. (2007) Snail, Zeb and bHLH factors in tumour progression: an alliance against the epithelial phenotype? *Nat Rev Cancer* 7, 415-428

5. Franci, C., Takkunen, M., Dave, N., Alameda, F., Gomez, S., Rodriguez, R., Escriva, M., Montserrat-Sentis, B., Baro, T., Garrido, M., Bonilla, F., Virtanen, I., and Garcia de Herreros, A. (2006) Expression of Snail protein in tumor-stroma interface. *Oncogene* 25, 5134-5144

6. Batlle, R., Alba-Castellon, L., Loubat-Casanovas, J., Armenteros, E., Franci, C., Stanisavljevic, J., Banderas, R., Martin-Caballero, J., Bonilla, F., Baulida, J., Casal, J. I., Gridley, T., and Garcia de Herreros, A. (2013) Snail1 controls TGF-beta responsiveness and differentiation of mesenchymal stem cells. *Oncogene* 32, 3381-3389

7. de Frutos, C. A., Dacquin, R., Vega, S., Jurdic, P., Machuca-Gayet, I., and Nieto, M. A. (2009) Snail1 controls bone mass by regulating Runx2 and VDR expression during osteoblast differentiation. *EMBO J* 28, 686-696

8. Larriba, M. J., Casado-Vela, J., Pendas-Franco, N., Pena, R., Garcia de Herreros, A., Berciano, M. T., Lafarga, M., Casal, J. I., and Munoz, A. (2010) Novel snail1 target proteins in human colon cancer identified by proteomic analysis. *PLoS One* 5, e10221

9. Cristobo, I., Larriba, M. J., de los Rios, V., Garcia, F., Munoz, A., and Casal, J. I. (2011) Proteomic analysis of 1alpha,25-dihydroxyvitamin D3 action on human colon cancer cells reveals a link to splicing regulation. *J Proteomics* 75, 384-397

10. Farmer, S. R. (2006) Transcriptional control of adipocyte formation. *Cell Metab* 4, 263-273

11. Green, H., and Kehinde, O. (1976) Spontaneous heritable changes leading to increased adipose conversion in 3T3 cells. *Cell* 7, 105-113

12. Lee, Y. H., Kim, S. H., Lee, Y. J., Kang, E. S., Lee, B. W., Cha, B. S., Kim, J. W., Song, D. H., and Lee, H. C. (2013) Transcription factor Snail is a novel regulator of adipocyte differentiation via inhibiting the expression of peroxisome proliferator-activated receptor gamma. *Cell Mol Life Sci* 70, 3959-3971

13. Ong, S. E., and Mann, M. (2007) Stable isotope labeling by amino acids in cell culture for quantitative proteomics. *Methods Mol Biol* 359, 37-52

14. Geiger, T., Wisniewski, J. R., Cox, J., Zanivan, S., Kruger, M., Ishihama, Y., and Mann, M. (2011) Use of stable isotope labeling by amino acids in cell culture as a spike-in standard in quantitative proteomics. *Nat Protoc* 6, 147-157

15. Spellman, D. S., Deinhardt, K., Darie, C. C., Chao, M. V., and Neubert, T. A. (2008) Stable isotopic labeling by amino acids in cultured primary neurons: application to brain-derived neurotrophic factor-dependent phosphotyrosine-associated signaling. *Mol Cell Proteomics* 7, 1067-1076

16. Wisniewski, J. R., Zougman, A., Nagaraj, N., and Mann, M. (2009) Universal sample preparation method for proteome analysis. *Nat Methods* 6, 359-362

17. Barderas, R., Mendes, M., Torres, S., Bartolome, R. A., Lopez-Lucendo, M., Villar-Vazquez, R., Pelaez-Garcia, A., Fuente, E., Bonilla, F., and Casal, J. I. (2013) In-depth characterization of the secretome of colorectal cancer metastatic cells identifies key proteins in cell adhesion, migration, and invasion. *Mol Cell Proteomics* 12, 1602-1620

18. Nguyen, H., Wood I.A., Hill M.M. (2012) A robust permutation test for quantitative SILAC proteomics experiments. *J. Integr. OMICS* 2, 80-93

19. Vizcaino, J. A., Deutsch, E. W., Wang, R., Csordas, A., Reisinger, F., Rios, D., Dianes, J. A., Sun, Z., Farrah, T., Bandeira, N., Binz, P. A., Xenarios, I., Eisenacher, M., Mayer, G., Gatto, L., Campos, A., Chalkley, R. J., Kraus, H. J., Albar, J. P., Martinez-Bartolome, S., Apweiler, R., Omenn, G. S., Martens, L., Jones, A. R., and Hermjakob, H. (2014) ProteomeXchange provides globally coordinated proteomics data submission and dissemination. *Nat Biotechnol* 32, 223-226

20. Babel, I., Barderas, R., Diaz-Uriarte, R., Martinez-Torrecuadrada, J. L., Sanchez-Carbayo, M., and Casal, J. I. (2009) Identification of tumor-associated

autoantigens for the diagnosis of colorectal cancer in serum using high density protein microarrays. *Mol Cell Proteomics* 8, 2382-2395

21. Herranz, N., Pasini, D., Diaz, V. M., Franci, C., Gutierrez, A., Dave, N., Escriva, M., Hernandez-Munoz, I., Di Croce, L., Helin, K., Garcia de Herreros, A., and Peiro, S. (2008) Polycomb complex 2 is required for E-cadherin repression by the Snail1 transcription factor. *Mol Cell Biol* 28, 4772-4781

22. Pelaez-Garcia, A., Barderas, R., Torres, S., Hernandez-Varas, P., Teixido, J., Bonilla, F., de Herreros, A. G., and Casal, J. I. (2013) FGFR4 role in epithelial-mesenchymal transition and its therapeutic value in colorectal cancer. *PLoS One* 8, e63695

23. Barderas, R., Bartolome, R. A., Fernandez-Acenero, M. J., Torres, S., and Casal, J. I. (2012) High expression of IL-13 receptor alpha2 in colorectal cancer is associated with invasion, liver metastasis, and poor prognosis. *Cancer Res* 72, 2780-2790

24. Huang da, W., Sherman, B. T., and Lempicki, R. A. (2009) Systematic and integrative analysis of large gene lists using DAVID bioinformatics resources. *Nat Protoc* 4, 44-57

25. Alba-Castellon, L., Batlle, R., Franci, C., Fernandez-Acenero, M. J., Mazzolini, R., Pena, R., Loubat, J., Alameda, F., Rodriguez, R., Curto, J., Albanell, J., Munoz, A., Bonilla, F., Ignacio Casal, J., Rojo, F., and Garcia de Herreros, A. (2014) Snail1 expression is required for sarcomagenesis. *Neoplasia* 16, 413-421

26. Tato, I., Bartrons, R., Ventura, F., and Rosa, J. L. (2011) Amino acids activate mammalian target of rapamycin complex 2 (mTORC2) via PI3K/Akt signaling. *J Biol Chem* 286, 6128-6142

27. Harris, T. E., Chi, A., Shabanowitz, J., Hunt, D. F., Rhoads, R. E., and Lawrence, J. C., Jr. (2006) mTOR-dependent stimulation of the association of eIF4G and eIF3 by insulin. *EMBO J* 25, 1659-1668

28. Zhang, H. H., Huang, J., Duvel, K., Boback, B., Wu, S., Squillace, R. M., Wu, C. L., and Manning, B. D. (2009) Insulin stimulates adipogenesis through the Akt-TSC2-mTORC1 pathway. *PLoS One* 4, e6189

29. Hermann-Kleiter, N., Gruber, T., Lutz-Nicoladoni, C., Thuille, N., Fresser, F., Labi, V., Schiefermeier, N., Warnecke, M., Huber, L., Villunger, A., Eichele, G.,

Kaminski, S., and Baier, G. (2008) The nuclear orphan receptor NR2F6 suppresses lymphocyte activation and T helper 17-dependent autoimmunity. *Immunity* 29, 205-216

30. Ahmed, M., and Gaffen, S. L. (2013) IL-17 inhibits adipogenesis in part via C/EBPalpha, PPARgamma and Kruppel-like factors. *Cytokine* 61, 898-905

31. Hermann-Kleiter, N., Meisel, M., Fresser, F., Thuille, N., Muller, M., Roth, L., Katopodis, A., and Baier, G. (2012) Nuclear orphan receptor NR2F6 directly antagonizes NFAT and RORgammat binding to the Il17a promoter. *J Autoimmun* 39, 428-440

32. Ruddy, M. J., Wong, G. C., Liu, X. K., Yamamoto, H., Kasayama, S., Kirkwood, K. L., and Gaffen, S. L. (2004) Functional cooperation between interleukin-17 and tumor necrosis factor-alpha is mediated by CCAAT/enhancer-binding protein family members. *J Biol Chem* 279, 2559-2567

33. Shen, F., Ruddy, M. J., Plamondon, P., and Gaffen, S. L. (2005) Cytokines link osteoblasts and inflammation: microarray analysis of interleukin-17- and TNF-alpha-induced genes in bone cells. *J Leukoc Biol* 77, 388-399

34. Zuniga, L. A., Shen, W. J., Joyce-Shaikh, B., Pyatnova, E. A., Richards, A. G., Thom, C., Andrade, S. M., Cua, D. J., Kraemer, F. B., and Butcher, E. C. (2010) IL-17 regulates adipogenesis, glucose homeostasis, and obesity. *J Immunol* 185, 6947-6959

35. Balani, D., Aeberli, D., Hofstetter, W., and Seitz, M. (2013) Interleukin-17A stimulates granulocyte-macrophage colony-stimulating factor release by murine osteoblasts in the presence of 1,25-dihydroxyvitamin D(3) and inhibits murine osteoclast development in vitro. *Arthritis Rheum* 65, 436-446

36. Kondo, M., Yamaoka, K., Sonomoto, K., Fukuyo, S., Oshita, K., Okada, Y., and Tanaka, Y. (2013) IL-17 inhibits chondrogenic differentiation of human mesenchymal stem cells. *PLoS One* 8, e79463

37. Li, L., Xie, X., Qin, J., Jeha, G. S., Saha, P. K., Yan, J., Haueter, C. M., Chan, L., Tsai, S. Y., and Tsai, M. J. (2009) The nuclear orphan receptor COUP-TFII plays an essential role in adipogenesis, glucose homeostasis, and energy metabolism. *Cell Metab* 9, 77-87

38. Xu, Z., Yu, S., Hsu, C. H., Eguchi, J., and Rosen, E. D. (2008) The orphan nuclear receptor chicken ovalbumin upstream promoter-transcription factor II is a critical regulator of adipogenesis. *Proc Natl Acad Sci U S A* 105, 2421-2426

39. Papp, D., Lenti, K., Modos, D., Fazekas, D., Dul, Z., Turei, D., Foldvari-Nagy, L., Nussinov, R., Csermely, P., and Korcsmaros, T. (2012) The NRF2-related interactome and regulome contain multifunctional proteins and fine-tuned autoregulatory loops. *FEBS Lett* 586, 1795-1802

40. Warnecke, M., Oster, H., Revelli, J. P., Alvarez-Bolado, G., and Eichele, G. (2005) Abnormal development of the locus coeruleus in Ear2(Nr2f6)-deficient mice impairs the functionality of the forebrain clock and affects nociception. *Genes Dev* 19, 614-625

41. Avram, D., Ishmael, J. E., Nevrivy, D. J., Peterson, V. J., Lee, S. H., Dowell, P., and Leid, M. (1999) Heterodimeric interactions between chicken ovalbumin upstream promoter-transcription factor family members ARP1 and ear2. *J Biol Chem* 274, 14331-14336

42. Albers, M., Kranz, H., Kober, I., Kaiser, C., Klink, M., Suckow, J., Kern, R., and Koegl, M. (2005) Automated yeast two-hybrid screening for nuclear receptor-interacting proteins. *Mol Cell Proteomics* 4, 205-213

43. Stark, C., Breitkreutz, B. J., Chatr-Aryamontri, A., Boucher, L., Oughtred, R., Livstone, M. S., Nixon, J., Van Auken, K., Wang, X., Shi, X., Reguly, T., Rust, J. M., Winter, A., Dolinski, K., and Tyers, M. (2011) The BioGRID Interaction Database: 2011 update. *Nucleic Acids Res* 39, D698-704

44. Jung, D. J., Sung, H. S., Goo, Y. W., Lee, H. M., Park, O. K., Jung, S. Y., Lim, J., Kim, H. J., Lee, S. K., Kim, T. S., Lee, J. W., and Lee, Y. C. (2002) Novel transcription coactivator complex containing activating signal cointegrator 1. *Mol Cell Biol* 22, 5203-5211

45. Prasad, T. S., Kandasamy, K., and Pandey, A. (2009) Human Protein Reference Database and Human Proteinpedia as discovery tools for systems biology. *Methods Mol Biol* 577, 67-79

46. Lee, Y. S., Kim, H. J., Lee, H. J., Lee, J. W., Chun, S. Y., Ko, S. K., and Lee, K. (2002) Activating signal cointegrator 1 is highly expressed in murine testicular Leydig cells and enhances the ligand-dependent transactivation of androgen receptor. *Biol Reprod* 67, 1580-1587

47. Iannone, M. A., Consler, T. G., Pearce, K. H., Stimmel, J. B., Parks, D. J., and Gray, J. G. (2001) Multiplexed molecular interactions of nuclear receptors using fluorescent microspheres. *Cytometry* 44, 326-337

48. Ocana, O. H., Corcoles, R., Fabra, A., Moreno-Bueno, G., Acloque, H., Vega, S., Barrallo-Gimeno, A., Cano, A., and Nieto, M. A. (2012) Metastatic colonization requires the repression of the epithelial-mesenchymal transition inducer Prrx1. *Cancer Cell* 22, 709-724

49. Xu, B., Gerin, I., Miao, H., Vu-Phan, D., Johnson, C. N., Xu, R., Chen, X. W., Cawthorn, W. P., MacDougald, O. A., and Koenig, R. J. (2010) Multiple roles for the non-coding RNA SRA in regulation of adipogenesis and insulin sensitivity. *PLoS One* 5, e14199

Table 1. *Function analysis of selected deregulated proteins in Snail-transfected cells*

			Foward SILAC				Reverse SILAC			
Function	**Accession no.**	**Name**	**Fold Change**	**Mascot Score**	**Coverage (%)**	**Peptides**	**Fold Change**	**Mascot Score**	**Coverage (%)**	**Peptides**
Chromatin remodelling	Q01320	Top2A	4.79	532.82	13.42	19	3.40	656.35	14.53	20
	P52927	Hmga2	1.73	9712.06	56.48	5	1.35	8936.29	45.37	4
Nuclear Transport	P62827	Ran	0.78	825.05	19.914	4	0.60	1929.96	30.56	7
	Q9EQK5	Mvp	0.34	134.54	4.07	3	0.07	233.79	11.38	7
	Q6P5F9	Xpo1	0.61	71.53	2.24	2	0.55	704.31	15.5	12
	Q9ERK4	Xpo2	0.20	259.36	3.50	3	0.30	1241.16	18.64	14
	Q924C1	Xpo5	0.33	112.11	3.57	4	0.26	517.33	8.97	8
	Q8BKC5	Ipo5	0.68	109.32	4.10	4	0.32	1525.89	16.13	13
Focal Adhesion	Q62523	Zyx	0.54	266.17	12.23	4	0.20	241.55	17.91	6
	P26039	Tln1	0.41	3557.29	16.10	28	0.32	12516.46	29	48
	Q71LX4	Tln2	0.46	801.25	6.40	12	0.72	1605.57	9.35	16
Transcription factors	Q80VJ2	Sra1	0.46	40.20	4.55	1	0.23	81.37	17.27	3
	P46938	Yap1	0.06	94.09	3.60	1	0.58	239.50	8.26	3
	P63013	Prrx1	0.75	781.09	14.69	3	0.40	746.62	18.37	4
	P43136	Nr2f6	0.63	123.91	10.77	3	0.53	62.52	6.67	2
	Q9QXN3	Trip4	0.78	34.74	2.24	1	0.45	44.68	1.38	1
	Q9DBY5	Cbx6	0.49	294.47	6.76	2	0.24	300.44	6.76	2
Cell Signaling	P62754	Rps6	0.65	3143.72	18.07	5	0.42	7588.44	21.29	6
	P42225	Stat1	0.43	85.41	5.07	3	0.72	116.28	3.2	2
	P42227	Stat3	0.68	328.73	10.26	5	0.21	513.22	13.25	6
	Q6A0A9	Fam120A	0.31	548.00	10.34	8	0.37	726.92	10.43	8
	O70458	OsmR	0.69	0.00	0.82	1	0.20	43.67	1.75	1
	Q63844	Erk1	0.41	448.89	17.11	5	0.40	595.95	21.58	6
	Q8BFW7	Lpp	0.28	114.53	15.33	6	0.27	41.48	7.18	3

Legends to the figures

Fig. 1. **Study of protein alterations in nuclear extracts of Snail1 transfected 3T3-L1 cells**. *A,* Verification of Snail1 overexpression in 3T3-L1 and mMSC cells by western blot analysis. *B,* 3T3-L1/Snail1 and 3T3-L1/Mock cells were analyzed at indicated cell confluence. The abundance of Snail1 and S100-A4 was quantified by western blot. Tubulin was used as loading control. According to the results, cell confluence was set up at 100% for 48h for the rest of the experiments. *C,* Schematic representation of proteomics experiments with 3T3-L1 cells. For metabolic labeling, 3T3-L1/Snail1 or control cells were grown and maintained in light and heavy-labeled DMEM medium supplemented with 10% dialyzed FBS. *D,* The quality of the subcellular fractionation was assessed by western blot before mass spectrometry. Cytoplasm and nuclear fractions were assayed using Lamin B and Rho GDI as nuclear and cytoplasmic protein controls, respectively. E, Proteins identified and quantified in 3T3-L1 forward and reverse SILAC experiments. In total, we identified 3920 proteins with 2800 overlapping proteins, whereas we quantified 3483 proteins with 2251 common proteins in both experiments. F, The enrichment of nuclear fraction with cellular component analyses was evaluated using DAVID Database. In total, 458 out of 2251 quantified proteins in 3T3-L1 were previously observed in nucleus.

Fig. 2. **Significant altered networks and pathways induced by Snail1.** *A,* Distribution of protein ratios versus protein abundance in Snail1 and control cells by SILAC analysis. Downregulated and upregulated proteins are indicated in black, red and blue, respectively. Unaltered proteins by Snail are represented in green. *B,* IPA database was used to identify the most significant altered pathways and biological functions due to

Snail1 overexpression in 3T3-L1 cells. *C,* IPA database predicted down-regulation of PPARγ and up-regulation of C/EBPβ mediators that are critical for the inhibition of final differentiation to adipocytes in 3T3-L1 cells.

Fig. 3. **Validation of Snail1-deregulated proteins in 3T3-L1 and mMSC cells by PCR and western blot**. *A,* cDNA synthesized from total RNA from 3T3-L1/Snail1 and control cells was subjected to semi-quantitative RT-PCR. *B,* Quantitative PCR analysis of Trip4, Nr2f6, OsmR, Prrx1, and CBX6 transcription factors in 3T3-L1/Snail1 and mMSC/Snail1 cells in comparison to control. Data represent the median and SD of three independent experiments. C, Nuclear protein extracts of 3T3-L1/Snail1, mMSC/Snail1 and control cells were subjected to western blot using specific antibodies against the indicated proteins. Lamin B was used as nuclear and loading control. D, 3T3-L1/Snail1 and control cells were transfected with the amplified promoters cloned in the pGL3 plasmid. E-cadherin promoter was used as control. Data represents the mean of Firefly luciferase ± SEM of three independent experiments performed on triplicate. **: $p < 0.005$; ***: $p < 0.001$ compared with control cells. E, To confirm the regulation of these transcription factors by Snail1, we performed ChIP assay using a specific anti-Snail1 antibody. PTEN was used as positive control of Snail1 regulation. An irrelevant IgG was used as negative control. Data represent the median/mean ± SD of the results. F, Western blot analysis of the reversion of the expression of the indicated transcription factors by knockdown of Snail1. Lamin B was used as loading control.

Fig. 4. **Adipocyte differentiation of 3T3-L1 cells is inhibited by silencing of Nr2f6 transcription factor.** *A,* 3T3-L1 preadipocytes were transfected with Trip4, Nr2f6,

Prrx1, CBX6 and control siRNA. On day 10 after treatment with adipogenic cocktail, cells were stained with Oil Red O. Photographs of differentiation were acquired with Olympus CK40 microscope equipped with an Olympus DP12 camera at x40 magnification. *B*, Oil Red O stained cells were dissolved in isopropanol and staining was quantified by absorbance at 500 nm. Data represents the mean ± SEM of three independent experiments performed on duplicate. *: $p < 0.01$; **: $p < 0.005$; ***: $p < 0.001$ compared with control cells. *C*, Western blot analysis of Nr2f6 knockdown. *D*, Western blot analysis of the expression levels of Nr2f6, and Snail1. RhoGDI was used as loading control. *E*, cDNA synthesized from total RNA from 3T3-L1/Snail1 and mock cells as control were subjected to qPCR analysis to amplify PPARγ, c/EBPα/β, Nr2f6 and Snail1. Murine ribosomal RNA 18S was used as control.

Fig. 5. **Enhanced expression of Nr2f6 reverts the effects of Snail1 and induced a fast adipocyte differentiation of 3T3-L1 cells.** *A*, 3T3-L1/Mock and 3T3-L1/Snail cells were transfected with pcDNA3.1/Nr2f6 or empty vector and analyzed by western Blot. *B*, cDNA from transfected cells was subjected to qPCR analysis for PPARγ, C/EBPα/β, Nr2f6 and Snail1. Murine ribosomal RNA 18S was used as control. *C*, Representative images of f 3T3-L1 cells transfected with pcDNA3.1/Nr2f6 or empty vector were recorded at indicated times with an Olympus CK40 microscope equipped with an Olympus DP12 camera at x40 magnification. *D*, Transfectants cells were stained with Oil Red O after 7 days of adypocite differentiation. Oil Red O stained cells were dissolved in isopropanol and staining was quantified by absorbance at 500 nm. Data represents the mean ± SEM of two independent experiments performed on triplicate. *: $p < 0.01$; **: $p < 0.005$; ***: $p < 0.001$ compared with control cells. *E*,

3T3-L1 proliferation was determined by MTT assays after 48 h of culture. Optical density was significantly decreased by Nr2f6 overexpression (***: $p < 0.001$, compared with 3T3-L1/Mock cells).

Fig. 6. **Expression of IL-17 in 3T3-L1 and mMSC cells overexpressing Snail1 and IL-17 effect on adipogenesis.** *A*, Murine cytokine antibody microarrays were incubated with the indicated conditioned medium. In both 3T3-L1 and mMSC cells, Snail1 promoted the expression of IL-17 and TNFα among other cytokines. Bar graph was calculated for each cytokine with the mean and SEM of replicated spots in the array. *B*, IL-17 expression is promoted through the inhibition of Nr2f6 transcription factor by Snail1. IL-17 expression was quantified by ELISA in the conditioned medium of Snail1stably transfected 3T3-L1, mock and mMSC cell lines. *C*, We quantified IL-17 expression in Nr2f6-silenced and ectopically-expressing cells. Nr2f6 expression induces variations in IL-17 expression levels. *D*, Adipocyte differentiation was performed in the presence or not of anti- IL17A antibody (500 ng/ml). Cells were stained with Oil Red O. Oil Red O stained cells were dissolved in isopropanol and staining was quantified by absorbance at 500 nm. Data represents the mean ± SEM of two independent experiments performed on triplicate. *: $p < 0.01$; **: $p < 0.005$; ***: $p < 0.001$ compared with control cells. Anti-IL-17 antibody was able to reverse the effects of Snail1 overexpression on adipocyte differentiation. Images were taken as above.

Fig. 7. **Snail1 role in adipocyte differentiation.** A model of the action of Snail in adipocyte differentiation. Snail1 overexpression down-regulates Nr2f6 expression, which in turn increases expression of IL-17. IL-17 up-regulates C/EBPβ and down-

regulates C/EBPα and PPARγ. In addition, Snail1 down-regulates Trip4, another candidate mediator, which also interacts with PPARγ. Nr2f2 represents a central node between Nr2f6 and Trip4. These interactions will require further investigation.

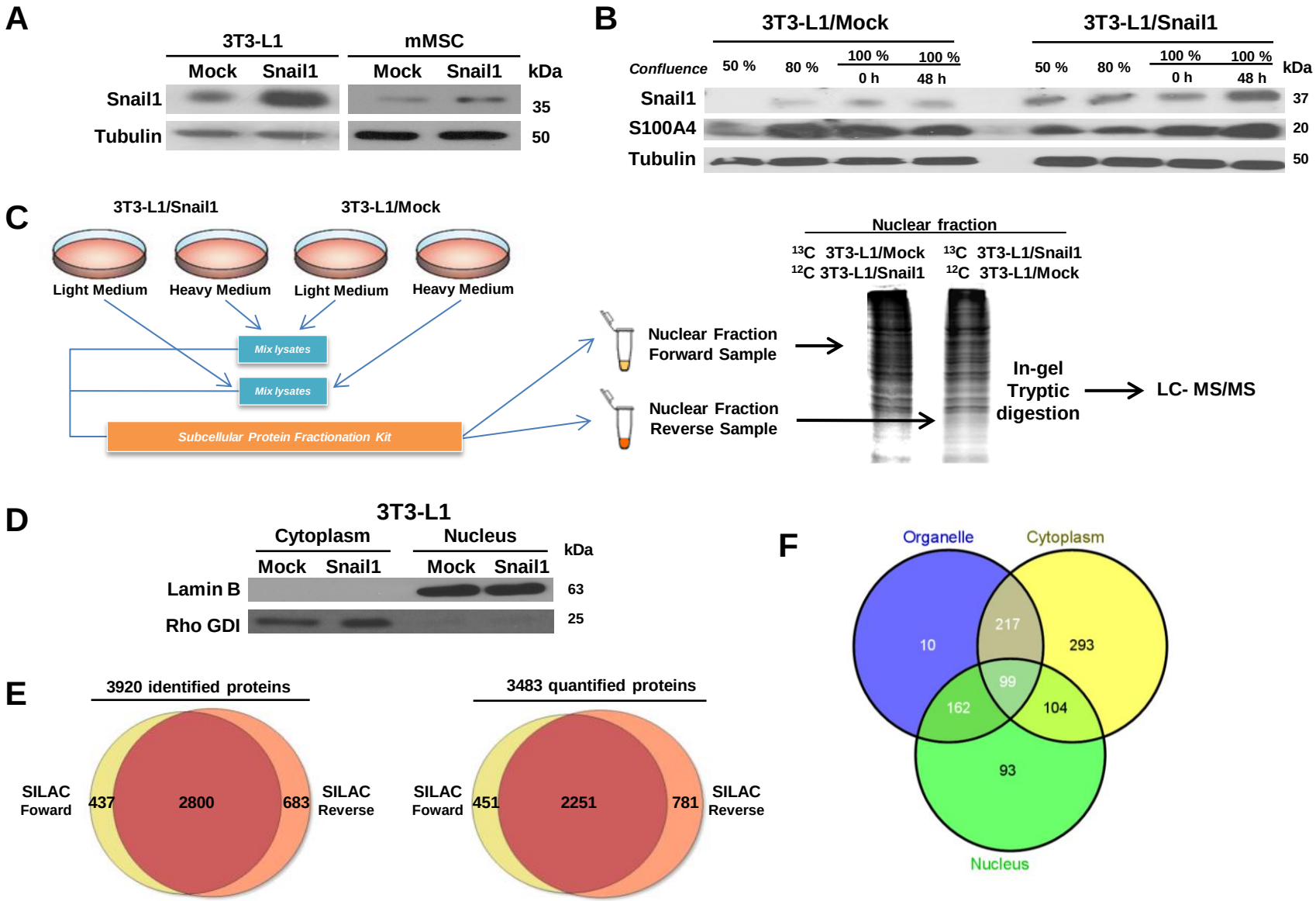
A
3T3-L1
mMSC
Mock
Snail1
Mock
Snail1
kDa
Snail1
Tubulin
35
50
B
3T3-L1/Mock
3T3-L1/Snail1
Confluence
50 %
80 %
100 %
0 h
100 %
48 h
50 %
80 %
100 %
0 h
100 %
48 h
kDa
Snail1
S100A4
Tubulin
37
20
50
C
3T3-L1/Snail1
3T3-L1/Mock
Light Medium
Heavy Medium
Light Medium
Heavy Medium
Mix lysates
Mix lysates
Subcellular Protein Fractionation Kit
Nuclear Fraction Forward Sample
Nuclear Fraction Reverse Sample
Nuclear fraction
13C 3T3-L1/Mock
12C 3T3-L1/Snail1
13C 3T3-L1/Snail1
12C 3T3-L1/Mock
In-gel Tryptic digestion
LC- MS/MS
D
3T3-L1
Cytoplasm
Nucleus
Mock
Snail1
Mock
Snail1
kDa
Lamin B
Rho GDI
63
25
E
3920 identified proteins
SILAC Foward
437
2800
683
SILAC Reverse
3483 quantified proteins
SILAC Foward
451
2251
781
SILAC Reverse
F
Organelle
Cytoplasm
Nucleus
10
217
293
99
162
104
93

Figure 1

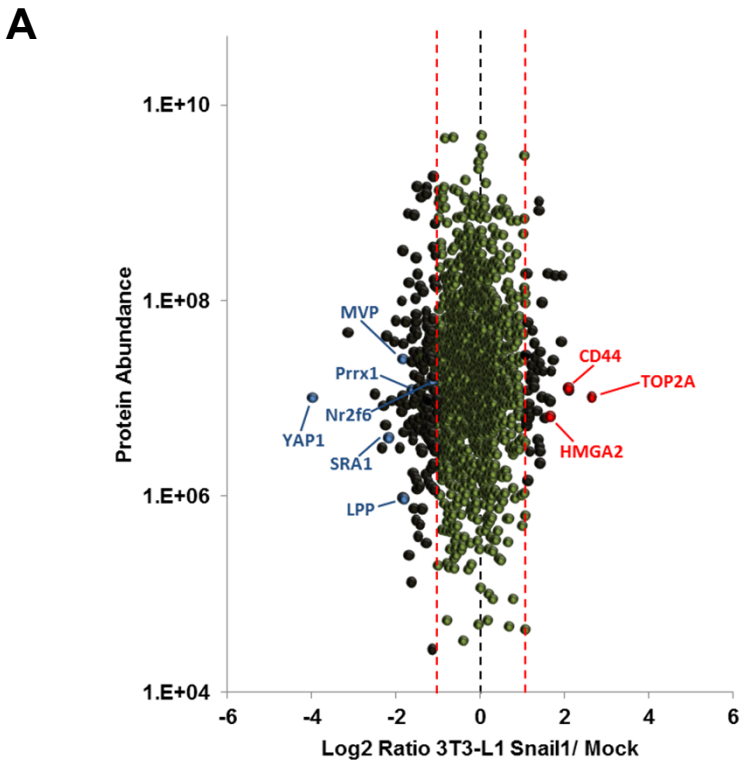
A
1.E+10
1.E+08
1.E+06
1.E+04
Protein Abundance
-6
-4
-2
0
2
4
6
Log2 Ratio 3T3-L1 Snail1/ Mock
MVP
Prrx1
Nr2f6
YAP1
SRA1
LPP
CD44
TOP2A
HMGA2

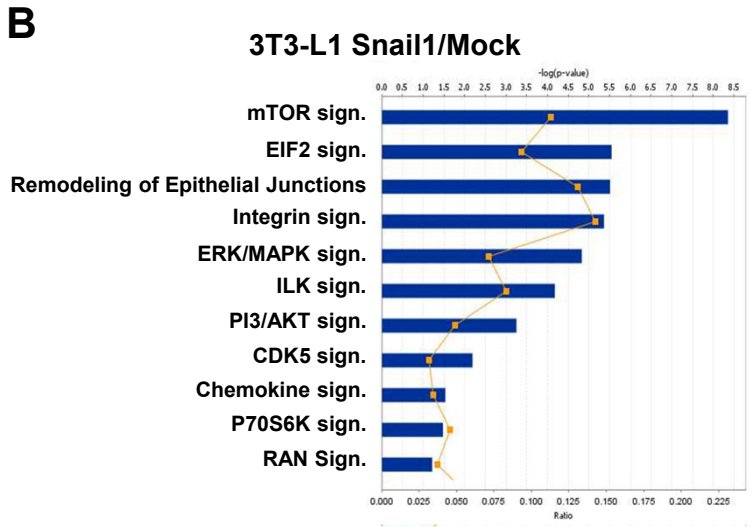
B
3T3-L1 Snail1/Mock
-log(p-value)
mTOR sign.
EIF2 sign.
Remodeling of Epithelial Junctions
Integrin sign.
ERK/MAPK sign.
ILK sign.
PI3/AKT sign.
CDK5 sign.
Chemokine sign.
P70S6K sign.
RAN Sign.
Ratio


C
Prediction Legend
Upregulated
Downregulated
Predicted activation
Predicted inhibition
Predicted Relationships
Leads to activation
Leads to inhibition
Findings inconsistent with state of downstream molecule
Effect not predicted
CXCL2
MMP14
PF4
LEP
IGFBP3
IL12B
CCL13
IL12A
DLK1
CXCL3*
IL10
IGFBP6
IL1B
TNF
CCL5
Plasma Membrane
VCAM1
ZYX
LEPR
Cytoplasm
FASN
VIM
HSD17B4
TKT
ACADL
FDPS
Ces1d
XDH
ERO1L
TUBB
ASNS
YWHAE
TPM2
Nucleus
PPARG
CEBPB
CTPS1
DHX9
DHFR

Figure 2

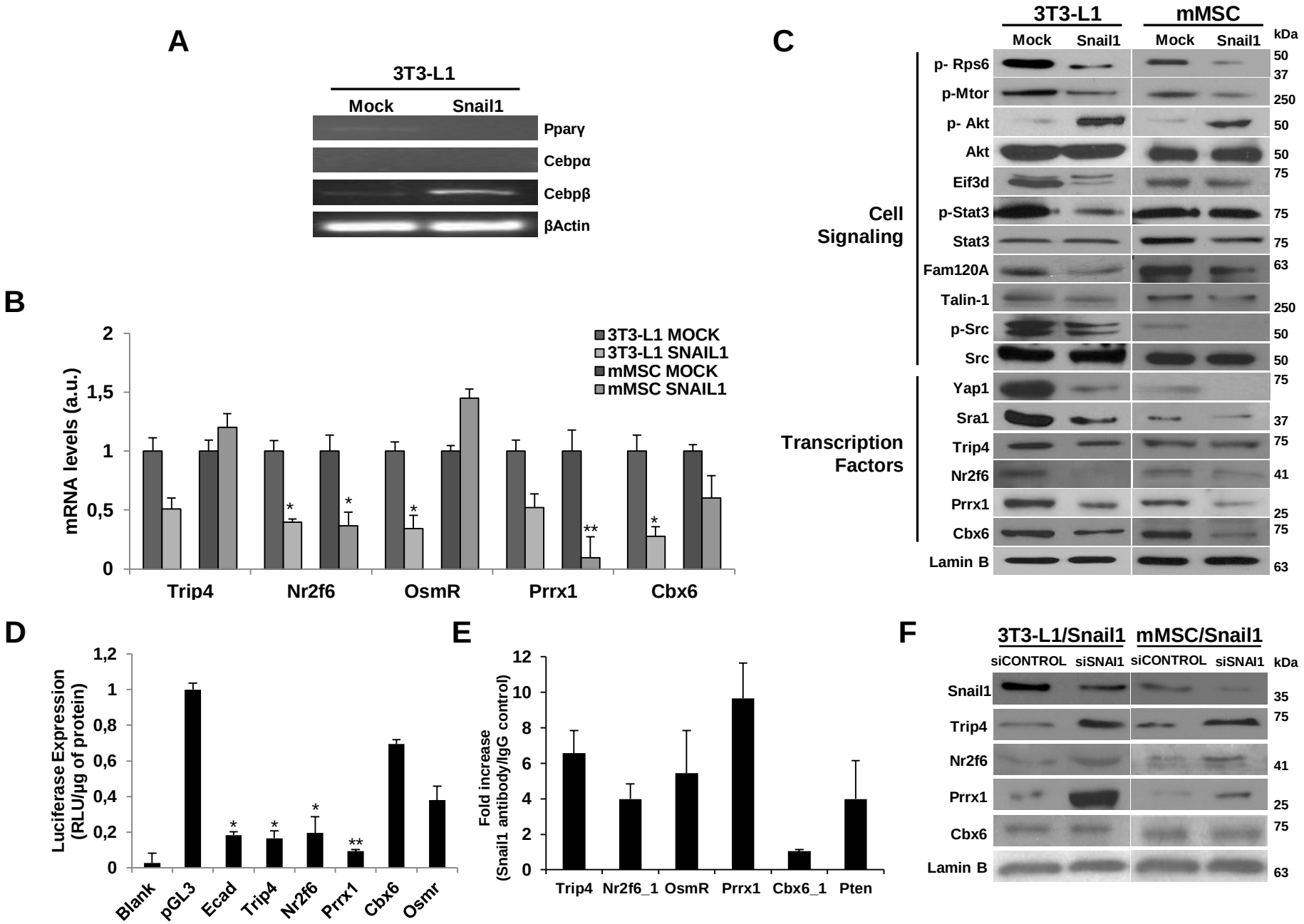
A
3T3-L1
Mock
Snail1
Pparγ
Cebpα
Cebpβ
βActin
B
mRNA levels (a.u.)
3T3-L1 MOCK
3T3-L1 SNAIL1
mMSC MOCK
mMSC SNAIL1
Trip4
Nr2f6
OsmR
Prrx1
Cbx6
C
3T3-L1
mMSC
Mock
Snail1
kDa
Cell Signaling
p- Rps6
p-Mtor
p- Akt
Akt
Eif3d
p-Stat3
Stat3
Fam120A
Talin-1
p-Src
Src
Transcription Factors
Yap1
Sra1
Trip4
Nr2f6
Prrx1
Cbx6
Lamin B
D
Luciferase Expression (RLU/µg of protein)
Blank
pGL3
Ecad
Trip4
Nr2f6
Prrx1
Cbx6
Osmr
E
Fold increase (Snail1 antibody/IgG control)
Trip4
Nr2f6_1
OsmR
Prrx1
Cbx6_1
Pten
F
3T3-L1/Snail1
mMSC/Snail1
siCONTROL
siSNAI1
kDa
Snail1
Trip4
Nr2f6
Prrx1
Cbx6
Lamin B

Figure 3

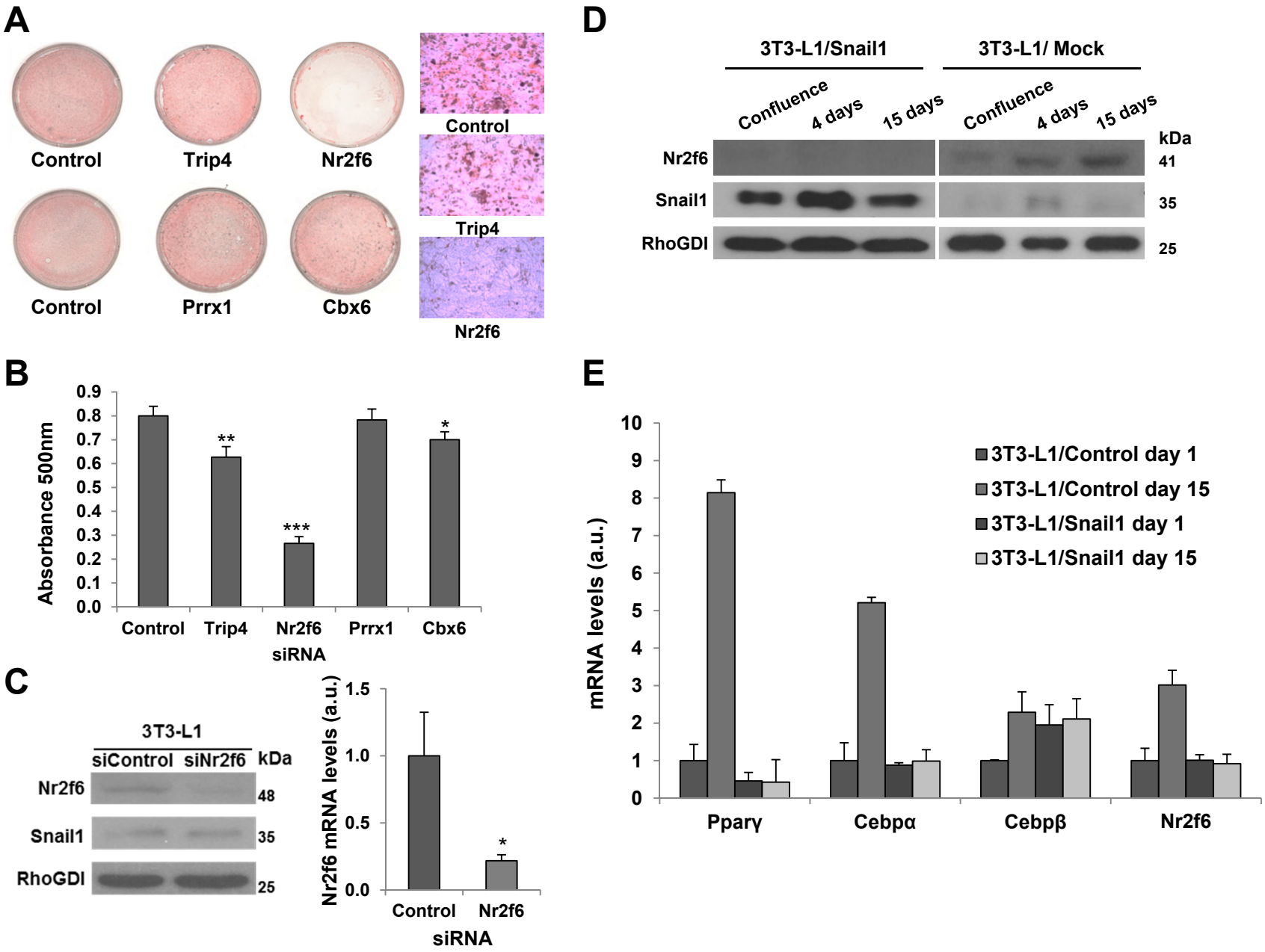
A
Control
Trip4
Nr2f6
Control
Prrx1
Cbx6
Control
Trip4
Nr2f6
B
Absorbance 500nm
0.9
0.8
0.7
0.6
0.5
0.4
0.3
0.2
0.1
0.0
**
***
*
Control
Trip4
Nr2f6
Prrx1
Cbx6
siRNA
C
3T3-L1
siControl
siNr2f6
kDa
Nr2f6
48
Snail1
35
RhoGDI
25
Nr2f6 mRNA levels (a.u.)
1.5
1.0
0.5
0.0
*
Control
Nr2f6
siRNA
D
3T3-L1/Snail1
3T3-L1/ Mock
Confluence
4 days
15 days
Confluence
4 days
15 days
kDa
Nr2f6
41
Snail1
35
RhoGDI
25
E
mRNA levels (a.u.)
10
9
8
7
6
5
4
3
2
1
0
3T3-L1/Control day 1
3T3-L1/Control day 15
3T3-L1/Snail1 day 1
3T3-L1/Snail1 day 15
Pparγ
Cebpα
Cebpβ
Nr2f6

Figure 4

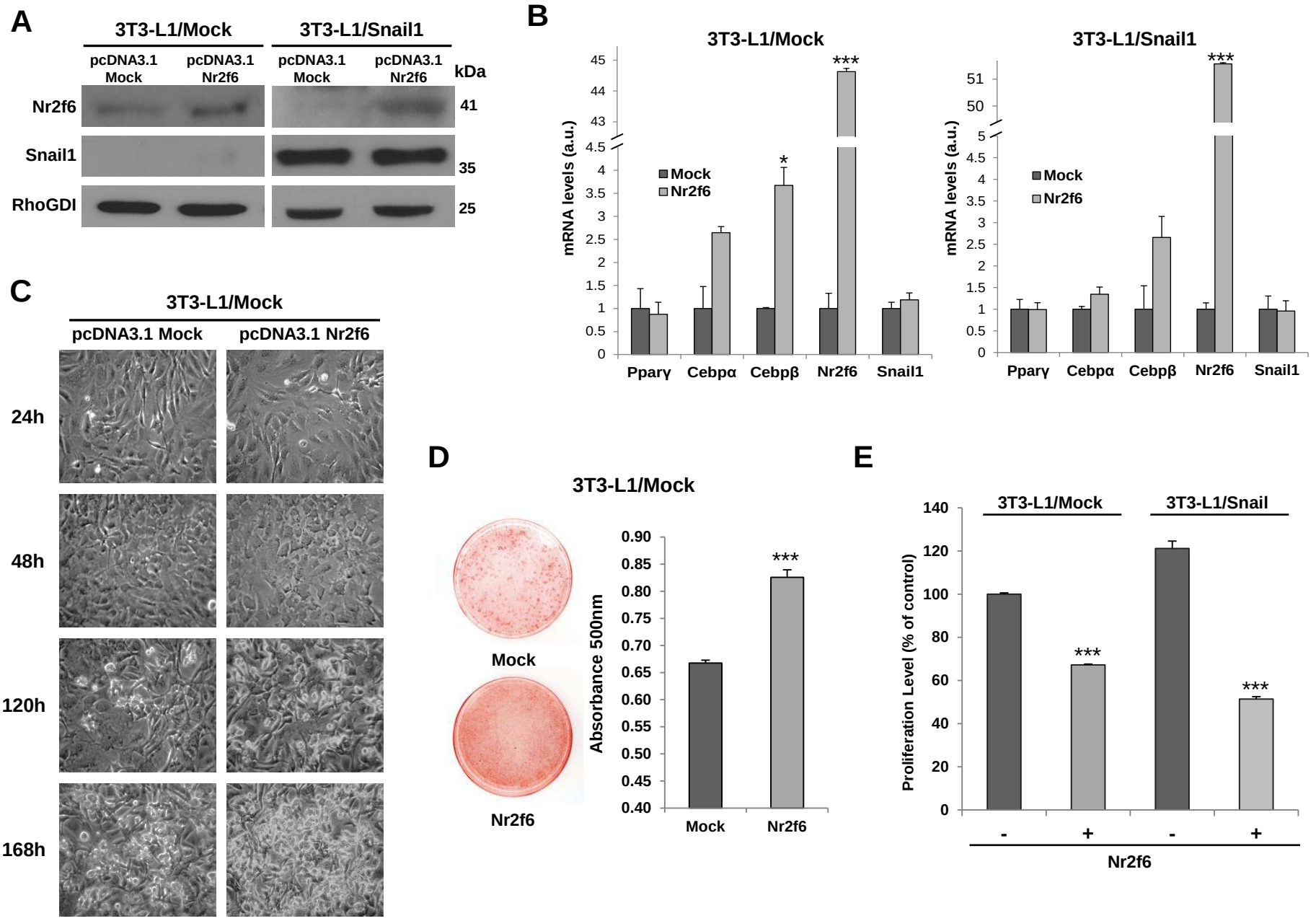
A
3T3-L1/Mock
3T3-L1/Snail1
pcDNA3.1 Mock
pcDNA3.1 Nr2f6
pcDNA3.1 Mock
pcDNA3.1 Nr2f6
kDa
Nr2f6
Snail1
RhoGDI
41
35
25
B
3T3-L1/Mock
3T3-L1/Snail1
mRNA levels (a.u.)
Mock
Nr2f6
*
***
***
Pparγ
Cebpα
Cebpβ
Nr2f6
Snail1
C
3T3-L1/Mock
pcDNA3.1 Mock
pcDNA3.1 Nr2f6
24h
48h
120h
168h
D
3T3-L1/Mock
Mock
Nr2f6
Absorbance 500nm
***
Mock
Nr2f6
E
3T3-L1/Mock
3T3-L1/Snail
Proliferation Level (% of control)
***
***
-
+
-
+
Nr2f6

Figure 5

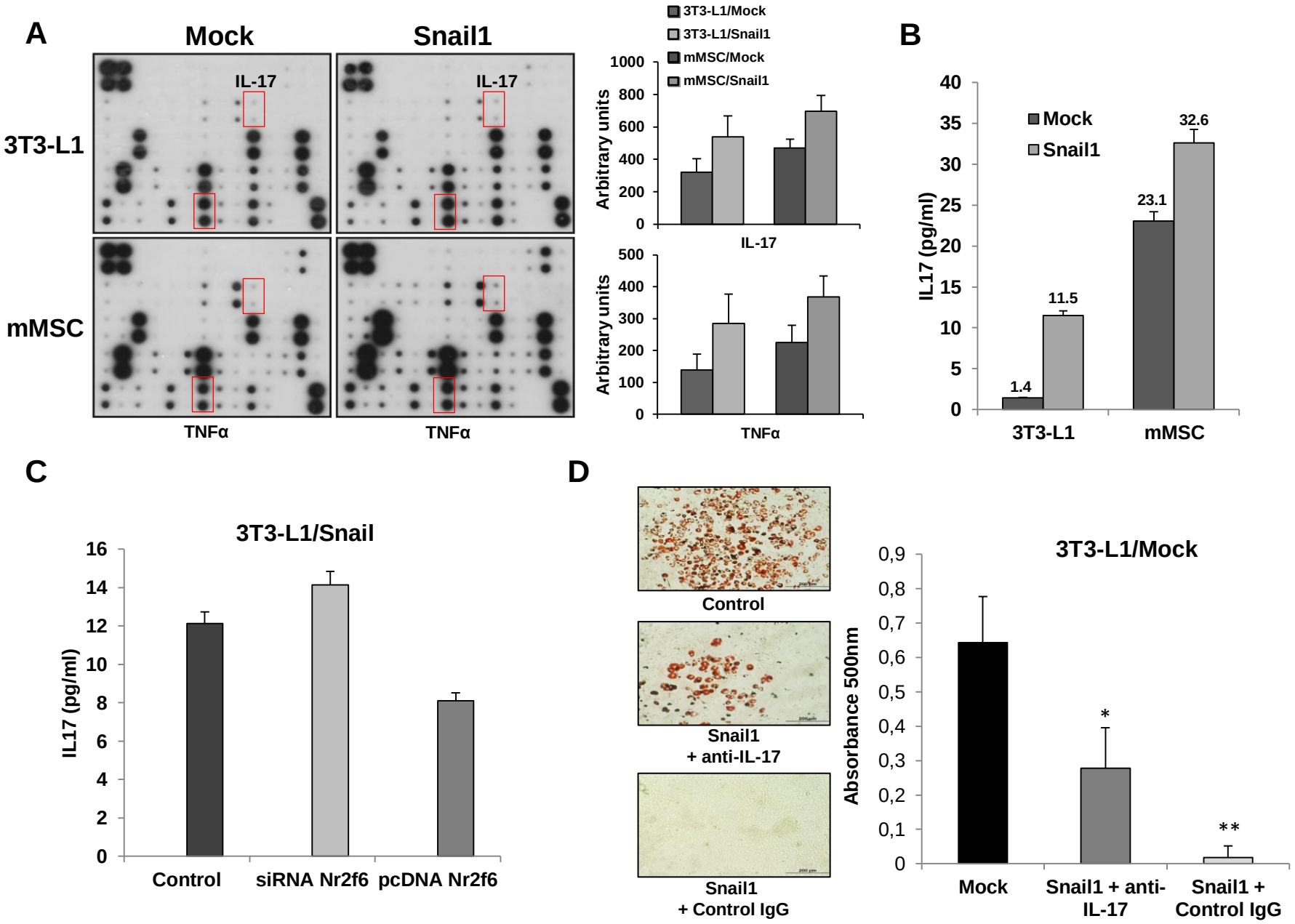
A
Mock
Snail1
3T3-L1
mMSC
IL-17
TNFα
3T3-L1/Mock
3T3-L1/Snail1
mMSC/Mock
mMSC/Snail1
Arbitrary units
B
Mock
Snail1
IL17 (pg/ml)
1.4
11.5
23.1
32.6
3T3-L1
mMSC
C
3T3-L1/Snail
IL17 (pg/ml)
Control
siRNA Nr2f6
pcDNA Nr2f6
D
Control
Snail1
+ anti-IL-17
Snail1
+ Control IgG
3T3-L1/Mock
Absorbance 500nm
Mock
Snail1 + anti-
IL-17
Snail1 +
Control IgG

Figure 6

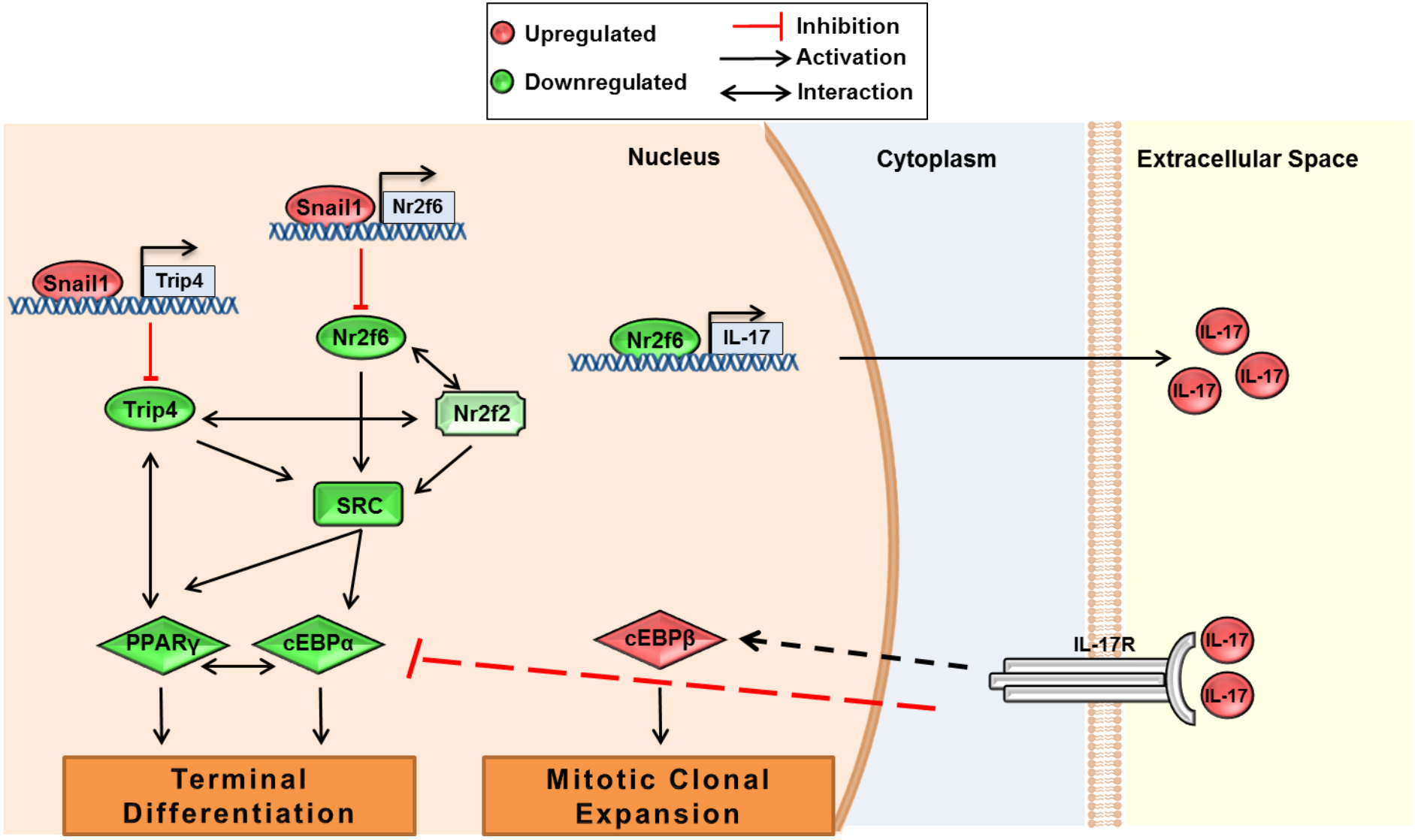
Upregulated
Downregulated
Inhibition
Activation
Interaction
Nucleus
Cytoplasm
Extracellular Space
Snail1
Nr2f6
Snail1
Trip4
Nr2f6
Trip4
Nr2f2
SRC
Nr2f6
IL-17
IL-17
IL-17
IL-17
PPARγ
cEBPα
cEBPβ
IL-17R
IL-17
IL-17
Terminal Differentiation
Mitotic Clonal Expansion

Figure 7